Supporting Information

Tuning Electronic Structure of Self-supported Vertically Aligned CoFe LDH Arrays Integrated with Ni Foam toward High Efficient Electrocatalytic Water Oxidation

Meng-Yang Li[a], Jun-Jun Zhang[a*], Xiang Li[a], Wei-Wei Bao[b], Chun-Ming Yang[c], Chang-Qing Jin[a], Meng Li[a], Su-Min Wang[a], Nan-Nan Zhang[d]

[a] School of Materials Science and Chemical Engineering, Xi'an Technological University, No.2 Xuefuzhonglu Road,Xi'an City,710021,China
E-mail: zhangjunjun@xatu.edu.cn
[b] National & Local Joint Engineering Laboratory for Slag Comprehensive Utilization and Environmental Technology, School of Material Science and Engineering, Shaanxi University of Technology, Hanzhong, Shaanxi, 723000 China
[c] Shaanxi Key Laboratory of Chemical Reaction Engineering, College of Chemistry & Chemical Engineering, Yan'an University, Yan'an 716000, China
[d] Instrumental Analysis Center, Shanghai Jiao Tong University, Shanghai 200240, China

Corresponding author.

E-mail address: zhangjunjun@xatu.edu.cn (J. J. Zhang).

List of Contents

1. Experimental details

1.1 Reagents

Cobalt (II) nitrate hexahydrate (AR), Urea(AR) were purchased from DAMAO. Iridium oxide (99.99%), Iron(II) chloride tetrachloride(98%) ammonium hydroxide(AR) and potassium hydroxide(AR) were obtained from ENERGY CHEMICAL,CMACKLIN KESHI and TIAN LI, respectively. These reagents were used without any purification. The ultrapure water (18.25MΩ·cm) was used through all the experiment process.

1.2 Preparation of Ni/CoFe LDH

The Ni/CoFe LDH self-supported vertically aligned electrode was synthesized by one-step electrodeposition. Ni foams (NF) were sonicated in diluted hydrochloric acid, ethanol and ultrapure water for 15min to clean the surface before used. The whole electrodeposition was carried out by using CHI660E Electrochemical Workstation (CHI Instruments, Shanghai, China) with saturated calomel (SCE) as reference electrode, platinum mesh as counter electrode and the cleaned NF as work electrode. A electrodeposition solution (40mL) contained 2.5mmol $Co(NO_3)_2 \cdot 6H_2O$ and 1.25mmol $FeCl_2 \cdot 4H_2O$ was firstly sonicated for 15min to accelerate dissolution and then 0.37mL ammonium hydroxide was added. The electrodeposition was conducted at a constant potential of -2.0 V vs. SCE. The deposition time was set as 100 (denoted as CoFe LDH-1), 200, 300s (denoted as CoFe LDH-3), respectively. The sample with 200s had best performance for OER, so denoted it as Ni/CoFe LDH and the loading amount was ~1.5mg cm^{-2}.

1.3 Preparation of CoFe LDH powder

The preparation process referred to the previous literature[1]. In detail, 30ml aqueous solution contained 0.25mmol $Co(NO_3)_2 \cdot 6H_2O$, 0.125mmol $FeCl_2 \cdot 4H_2O$, and 6mmol Urea was sonicated for 15min at room temperature. Then, the solution was transferred into a 50 ml Teflon-lined stainless steel autoclave, which was sealed and maintained at 140°C for 12h.

1.4 Preparation of (Ni + IrO2) and (Ni +CoFe LDH)

Prior to the synthesis, NF was sonicated in diluted hydrochloric acid, ethanol and ultrapure water for 15min to clean the surface. (Ni+IrO_2) was prepared as follows.

1.5mg IrO_2 was dispersed into a solution of water, ethanol and Nafion mixed system. The electrode was prepared by coating the Ni foam with dispersion solution. As for Ni +CoFe LDH electrode, the synthesis is same as the Ni +IrO_2 except for replacing IrO_2 with CoFe LDH powder. IrO_2 with CoFe LDH powder, which was the one used to compare OER performance as described above.

1.5 Characterizations

X-ray diffraction (XRD) pattern was obtained from SHIMADZU XRD6000 X-ray diffractometer with Cu Kα radiation (40 kV, 30 mA, λ = 1.5406 Å). The scan range (2 Theta) was 10-80˚ and scan speed was 4˚/ min. The SEM measurements were performed on ascanning electron microscope (FE-SEM, JSM-7610F, 10 kV). The TEM and HRTEM measurements were taken with a JEOL JEM-F200 microscope operated. The samples were prepared by dropping ethanol dispersion of samples onto carbon-coated copper TEM grids using pipettes and dried under ambient condition. The X-ray photoelectron spectroscopy (XPS) measurements were conducted on a Kratos Axis Ultra DLD spectrometer. The Raman spectra was acquired by the LabRAM HR Evolution Raman spectrometer with 532 nm excitation wavelength.

1.6 Electrochemical measurements

All electrochemical tests were performed in a conventional three-electrode system with a CHI-660E electrochemical workstation (CHI Instruments, Shanghai, China) at room temperature. As-prepared Ni/CoFe LDH electrodes, carbon rod, saturated calomel and 1M KOH were used as work electrodes, counter electrode, reference electrode and electrolyte, respectively. All linear sweep voltammetry (LSV) curves towards OER in this work were conducted at a scan rate of 10mV/s and calibrated by iR corrected. Electrochemical impedance spectroscopy (EIS) was measured in the same three-electrodes with AC impedance over a frequency range from 0. 1 to 10^5 Hz. The overpotential is defined according to η (mV) = (E (vs. RHE) – 1.23)*1000. The potentials used in this work were calibrated to RHE other than especially explained by the equation: E (vs. RHE) = E (vs. SCE) + 0.241 + 0.059 pH.

2. Supplementary Figures

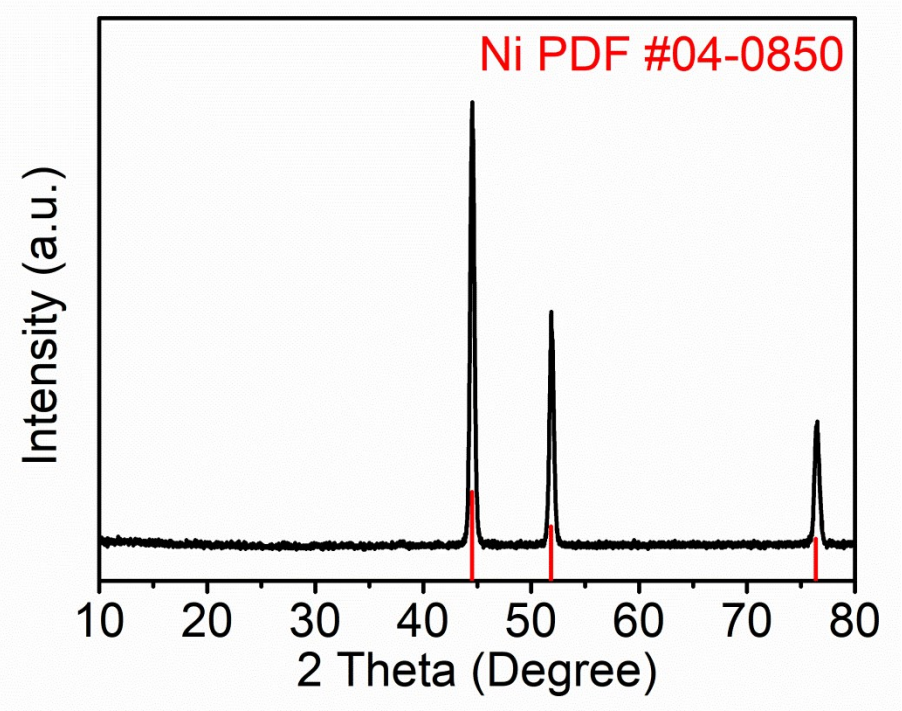

Figure S1. The XRD pattern of the Ni/CoFe LDH electrode and the standard card of Ni.

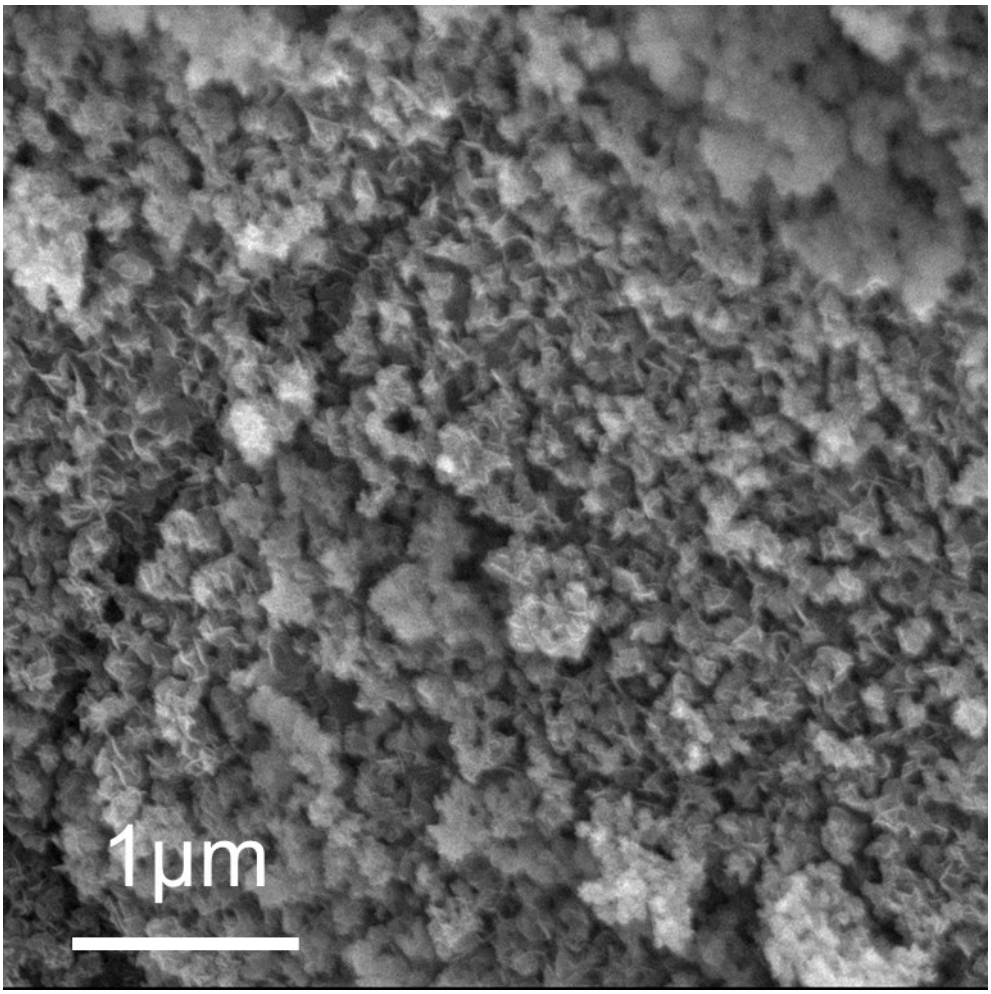

Figure S2. The low-resolution SEM of the Ni/CoFe LDH electrode.

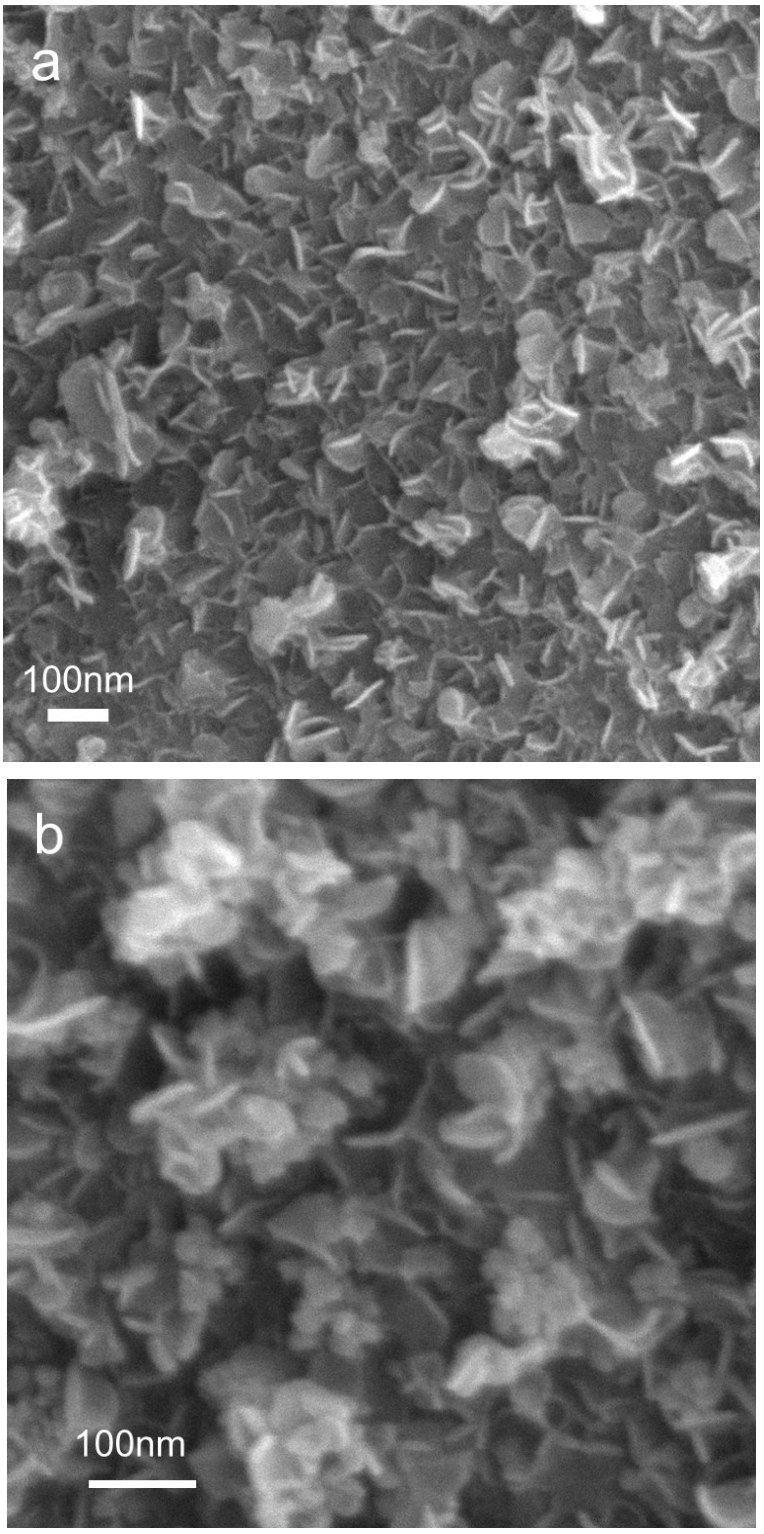

Figure S3. The high resolution SEM of Ni/CoFe LDH with different magnification: (a)×50000;(b)×100000.

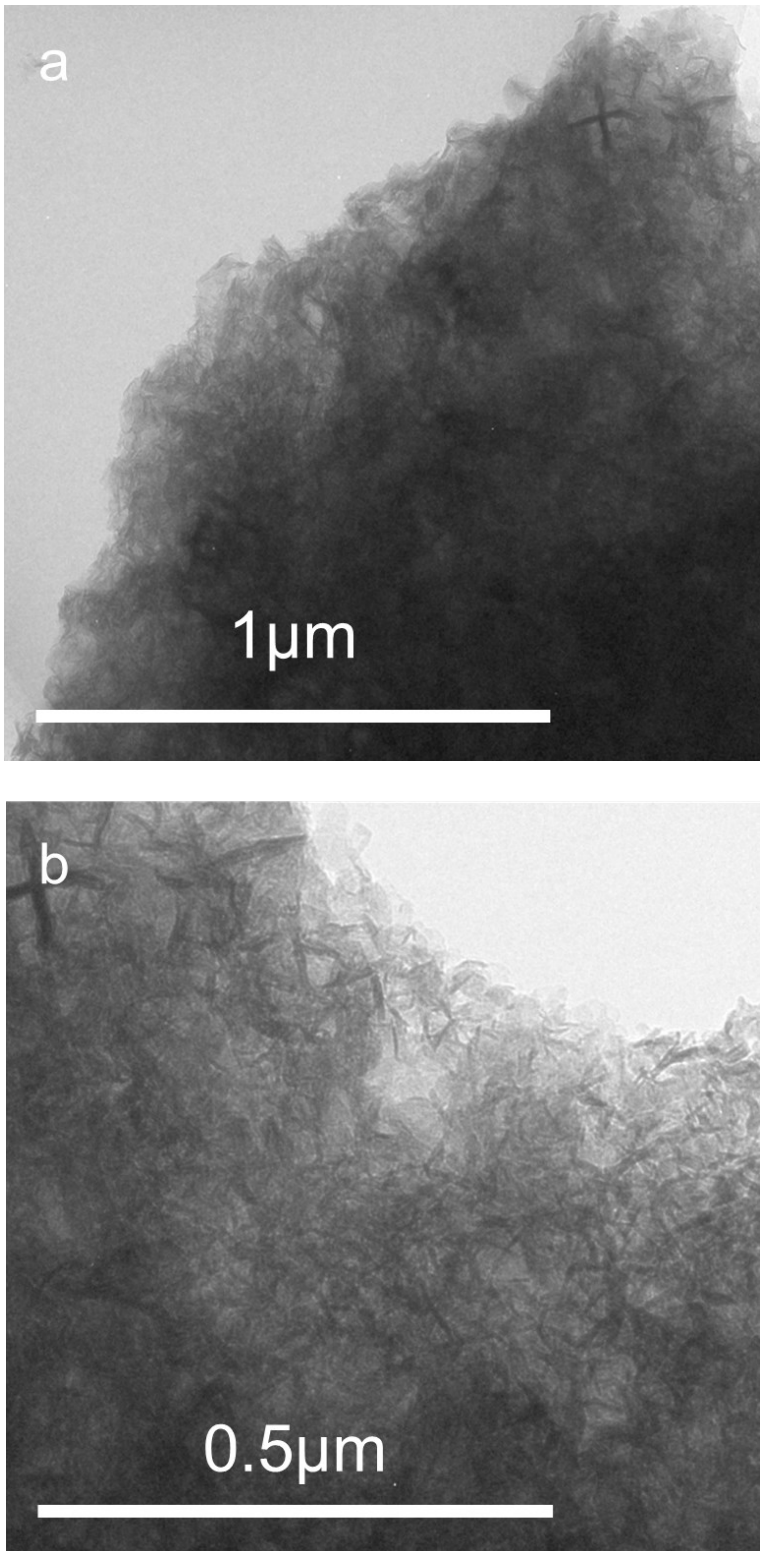

Figure S4. The low resolution TEM of Ni/CoFe LDH with different magnification.

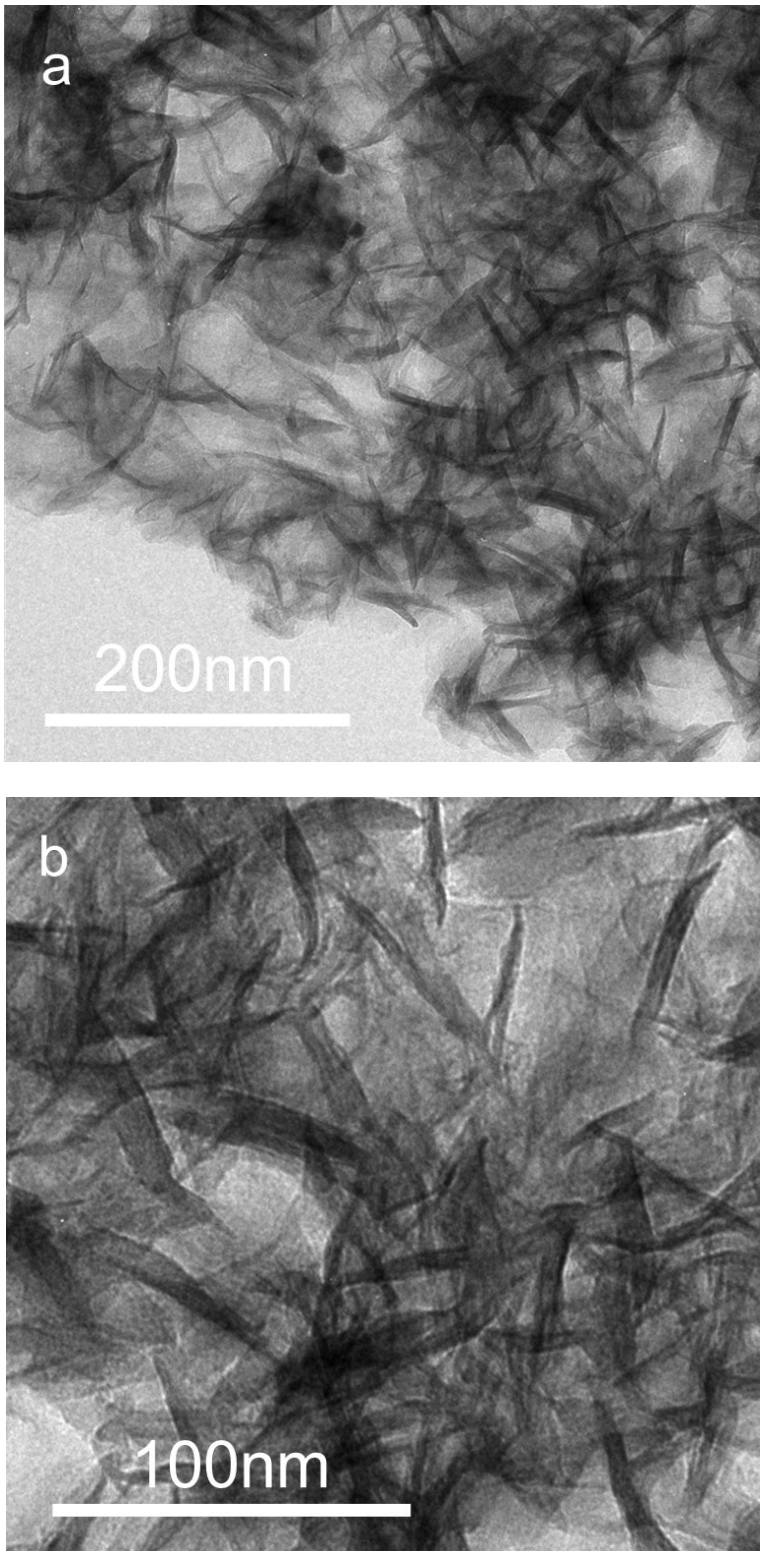

Figure S5. The high resolution TEM of Ni/CoFe LDH electrode with different magnification.

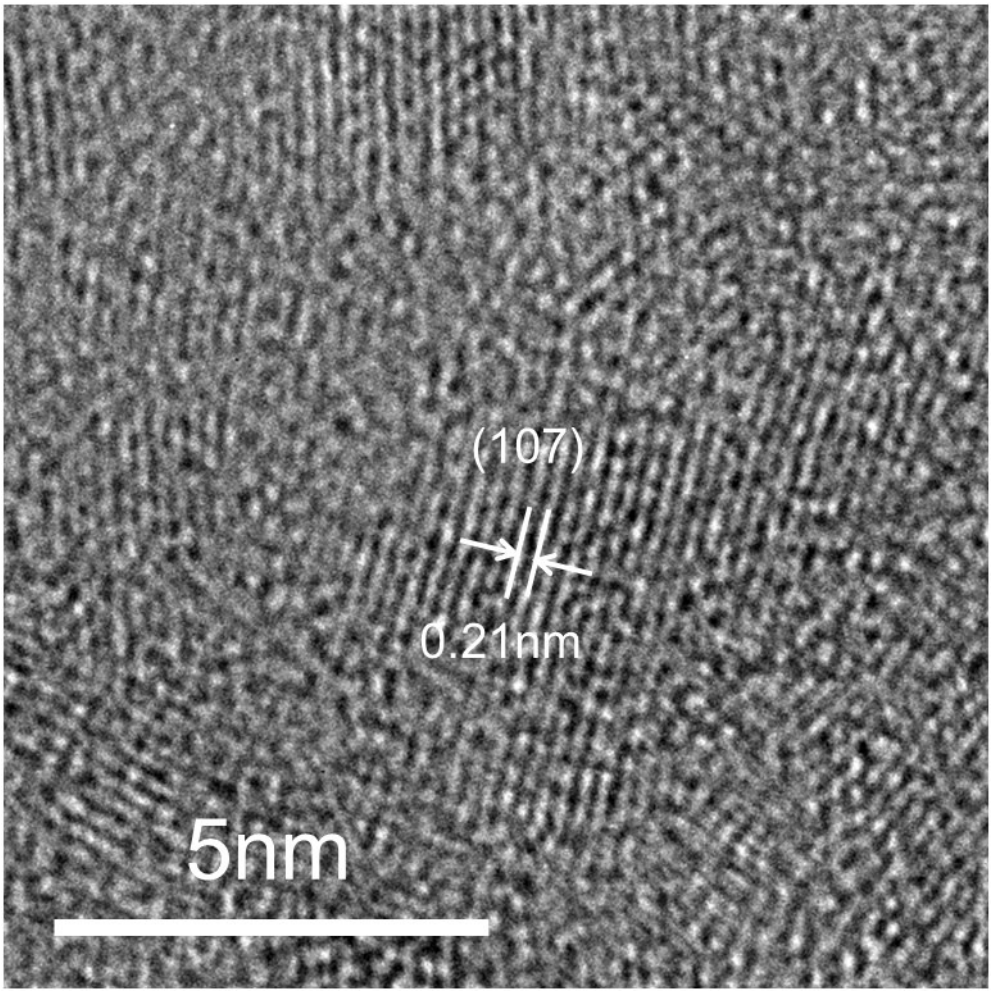

Figure S6. The HRTEM image of Ni/CoFe LDH electrode.

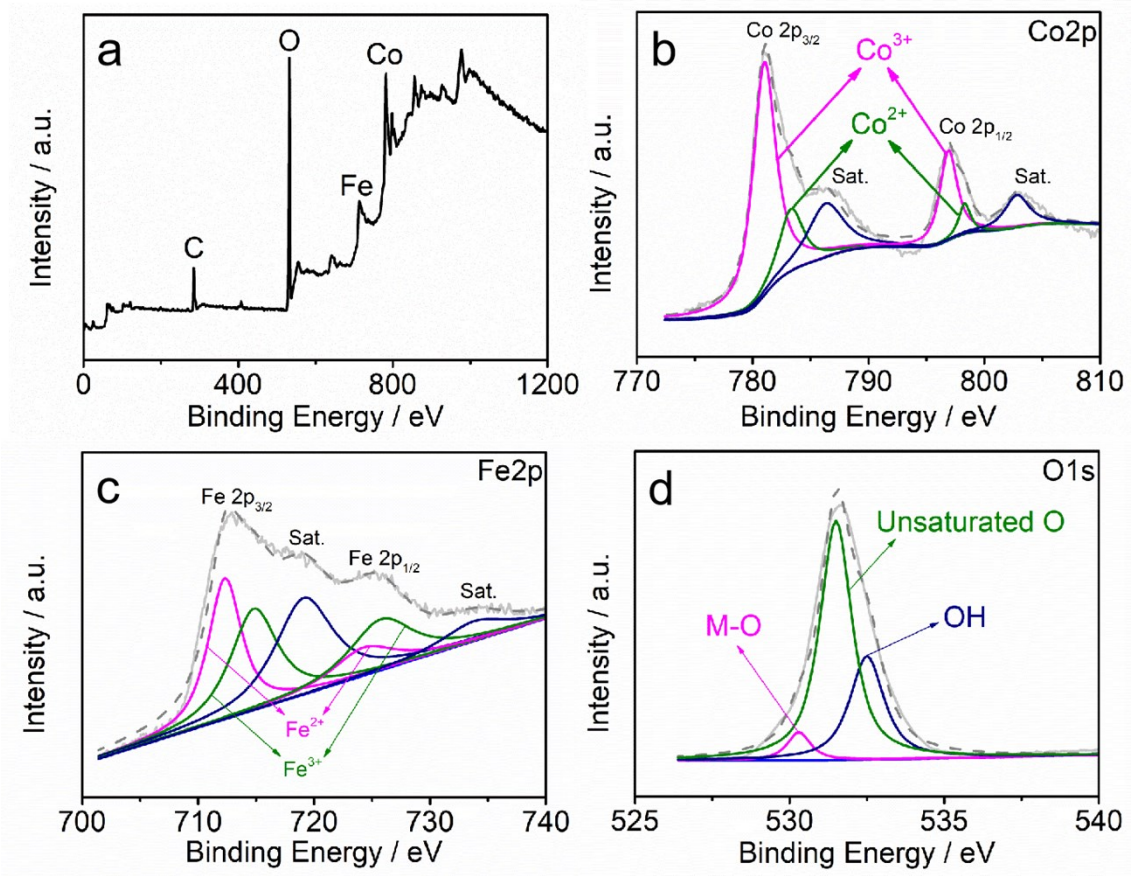

Figure S7. XPS spectra of Ni/CoFe LDH: (a) survey, (b) Co 2p, (c) Fe 2p, and (d) O 1s.

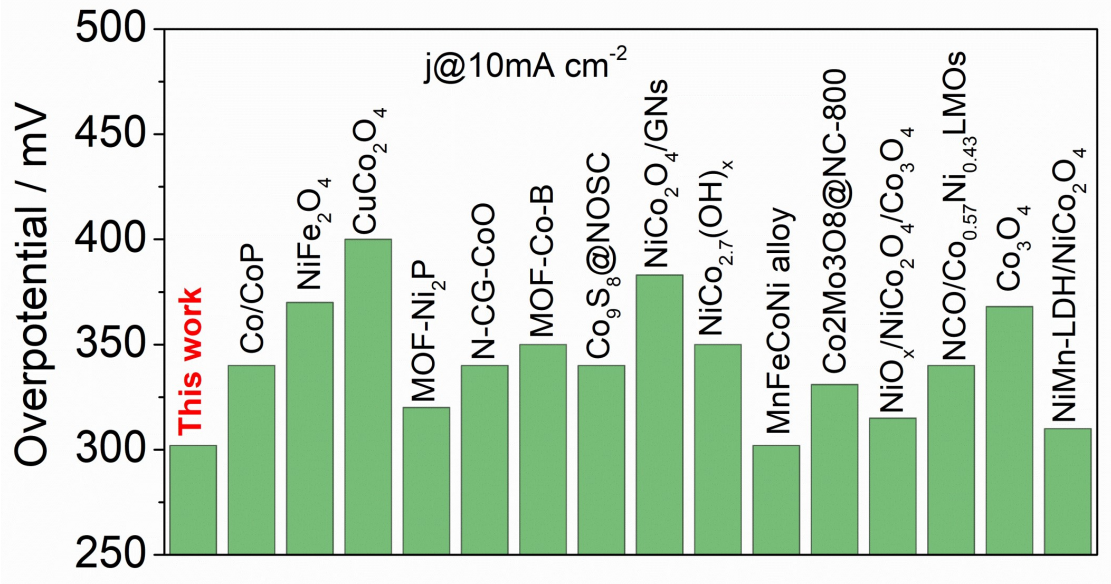

Figure S8. The comparison of OER performance for some representative non-noble electrocatalysts.

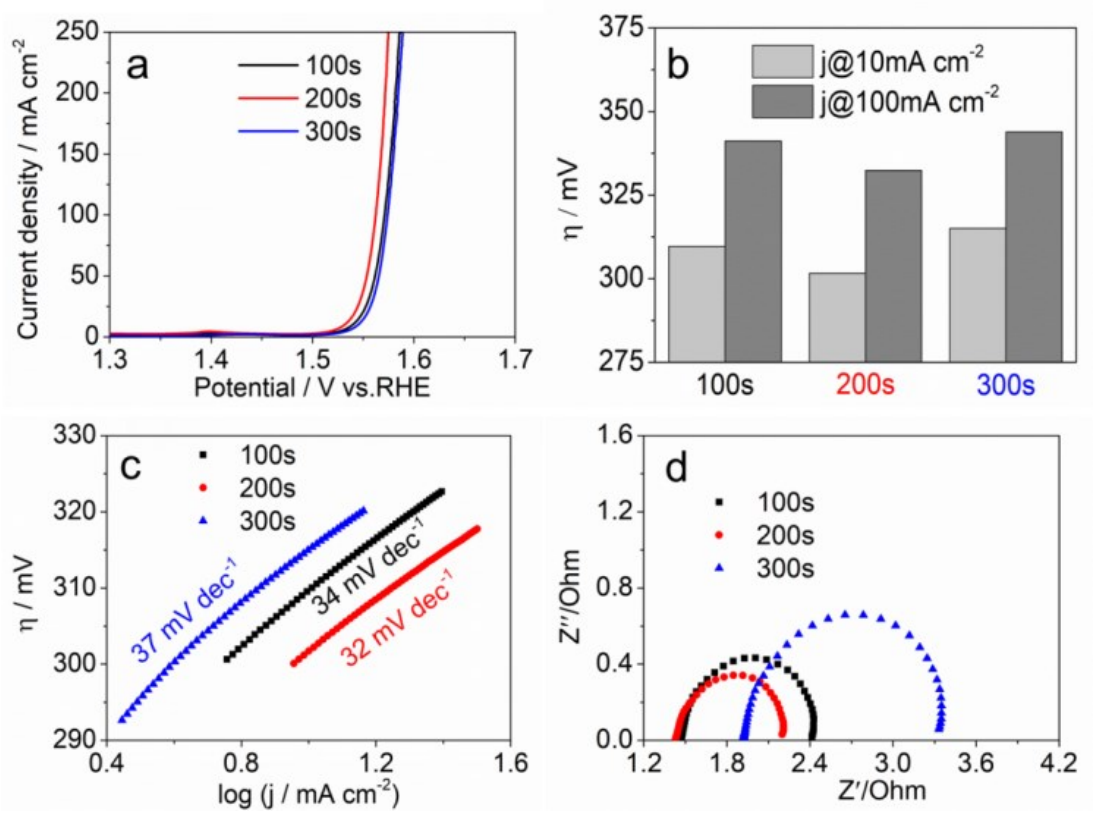

Figure S9. (a) The polarization curve, (b) the comparison of overpotential at 10 and 100 mA cm^{-2} current density, (c) the Tafel slope and (d) the electrochemical impedance spectra of CoFe LDH catalysts with different deposition time.

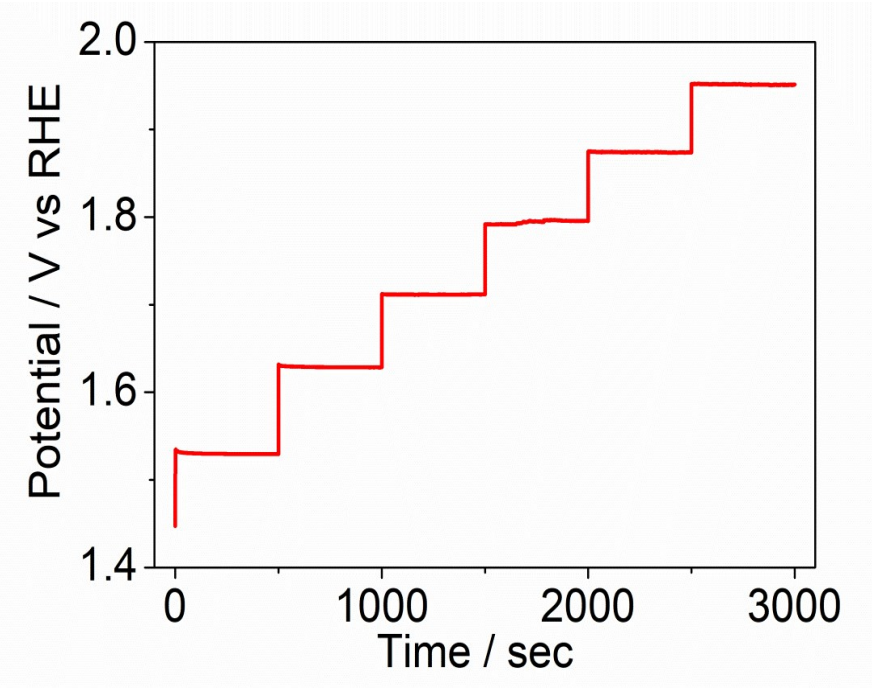

Figure S10. The multi-current steps of Ni/CoFe LDH catalysts.

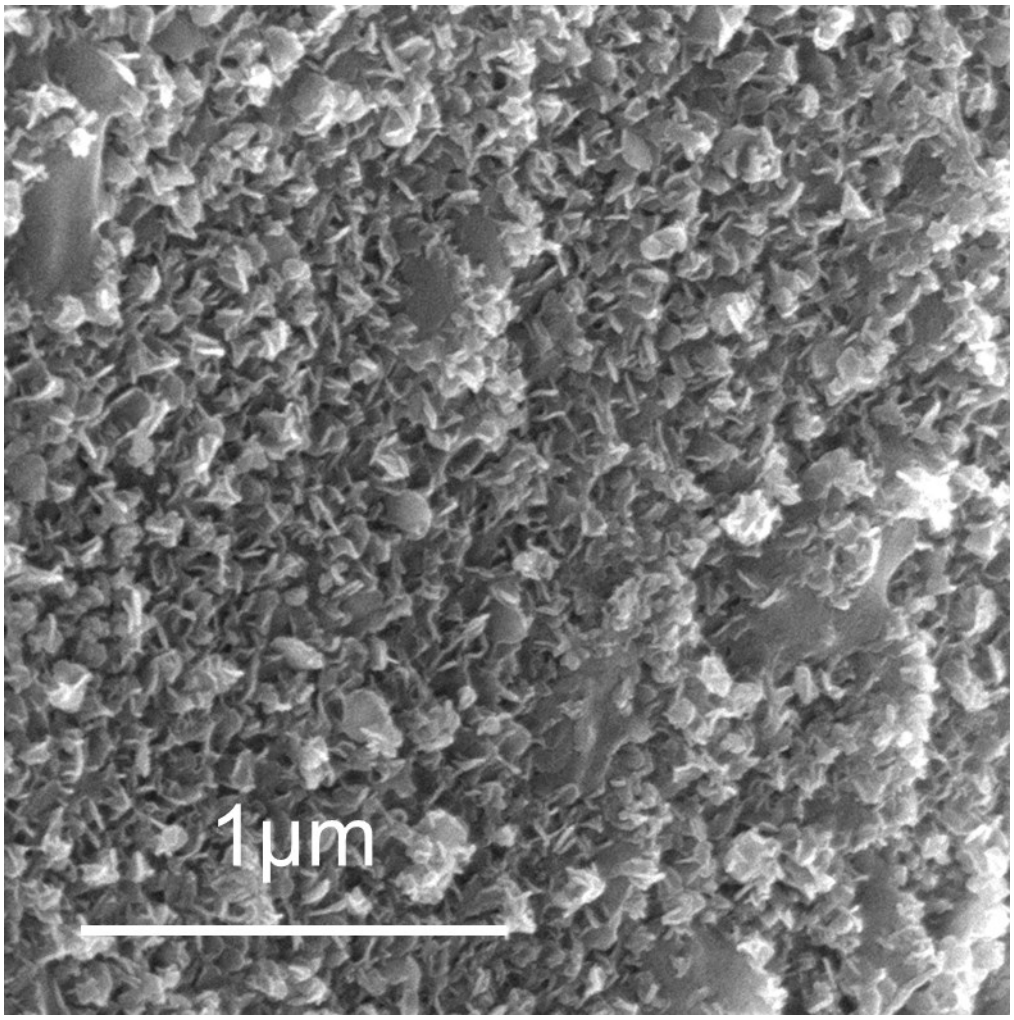

Figure S11. The low resolution SEM of Ni/CoFe LDH after OER test.

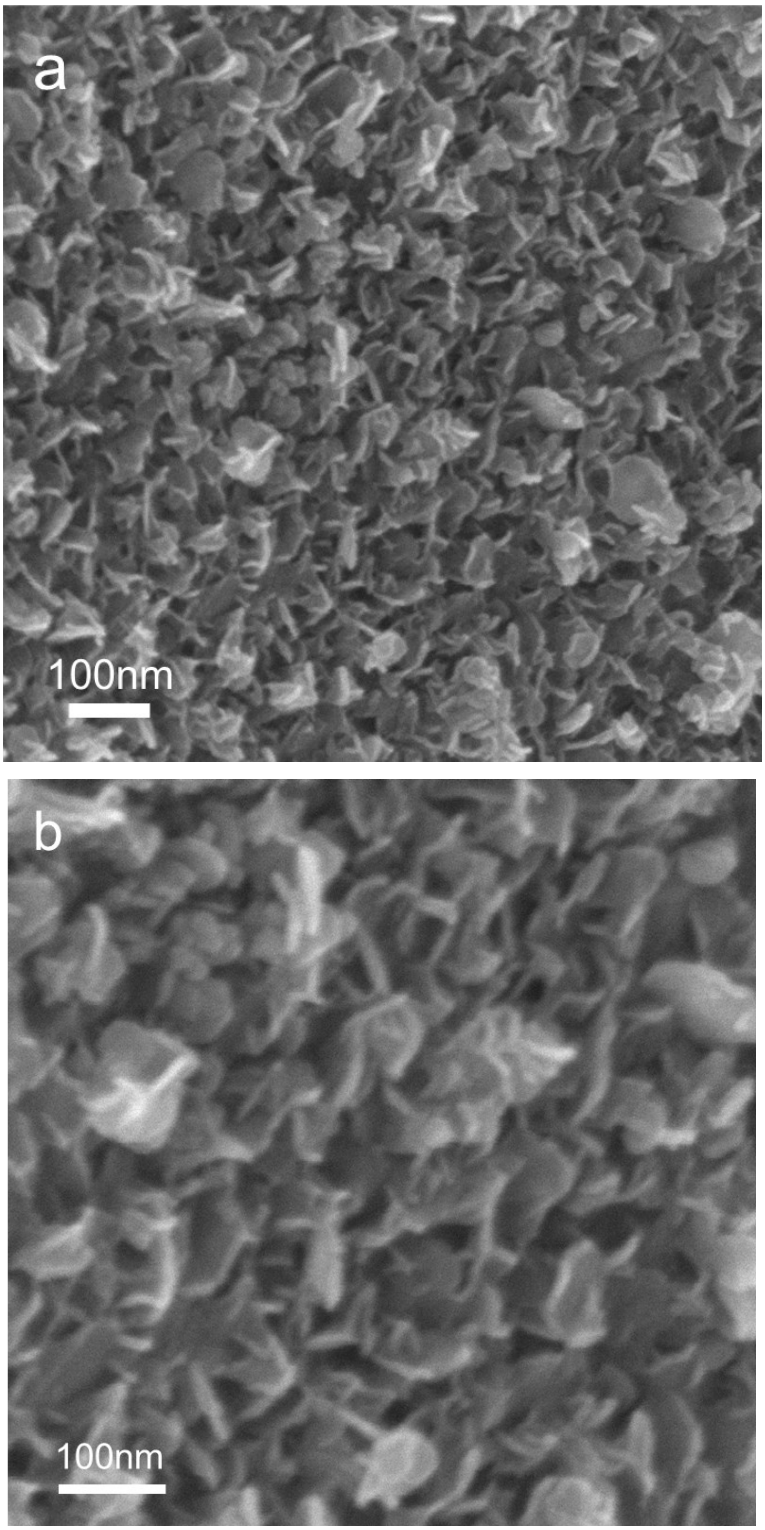

Figure S12. The high resolution SEM of Ni/CoFe LDH after OER test with different magnification: (a)×50000;(b)×100000.

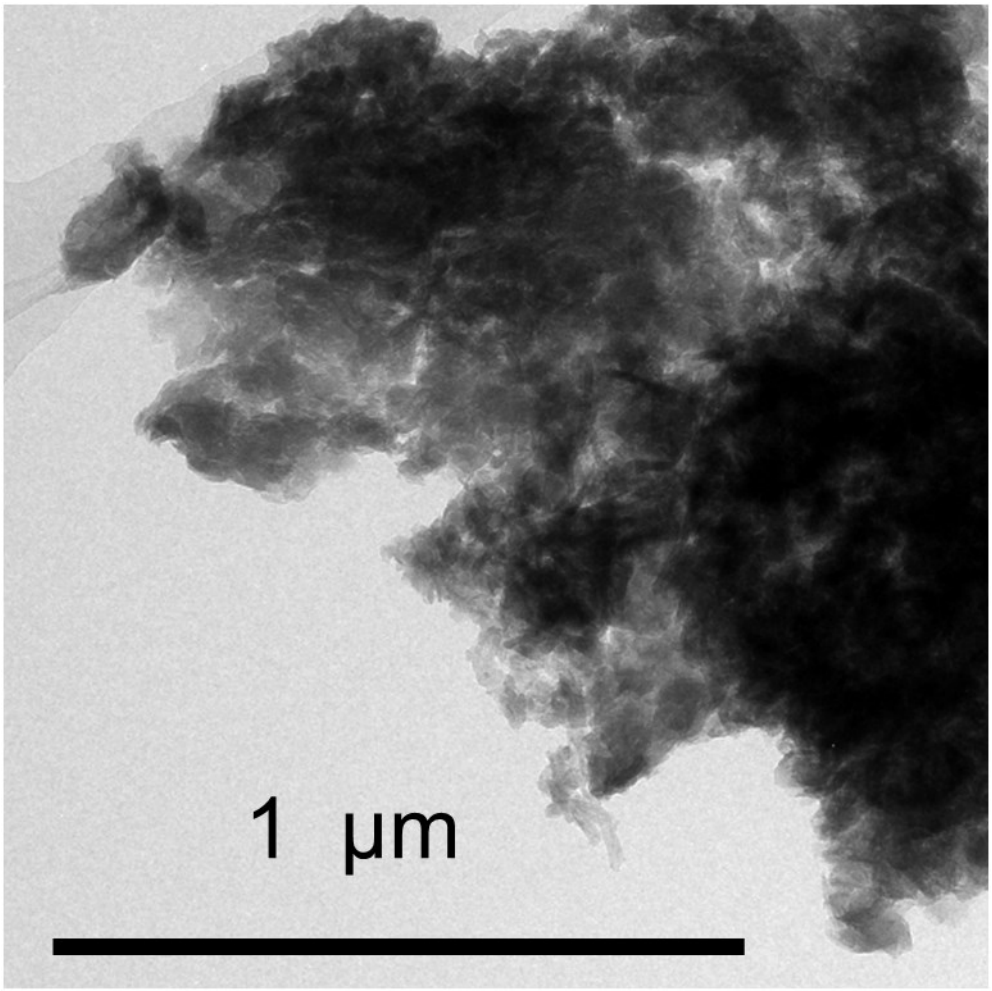

Figure S13. The low resolution TEM of Ni/CoFe LDH after OER test.

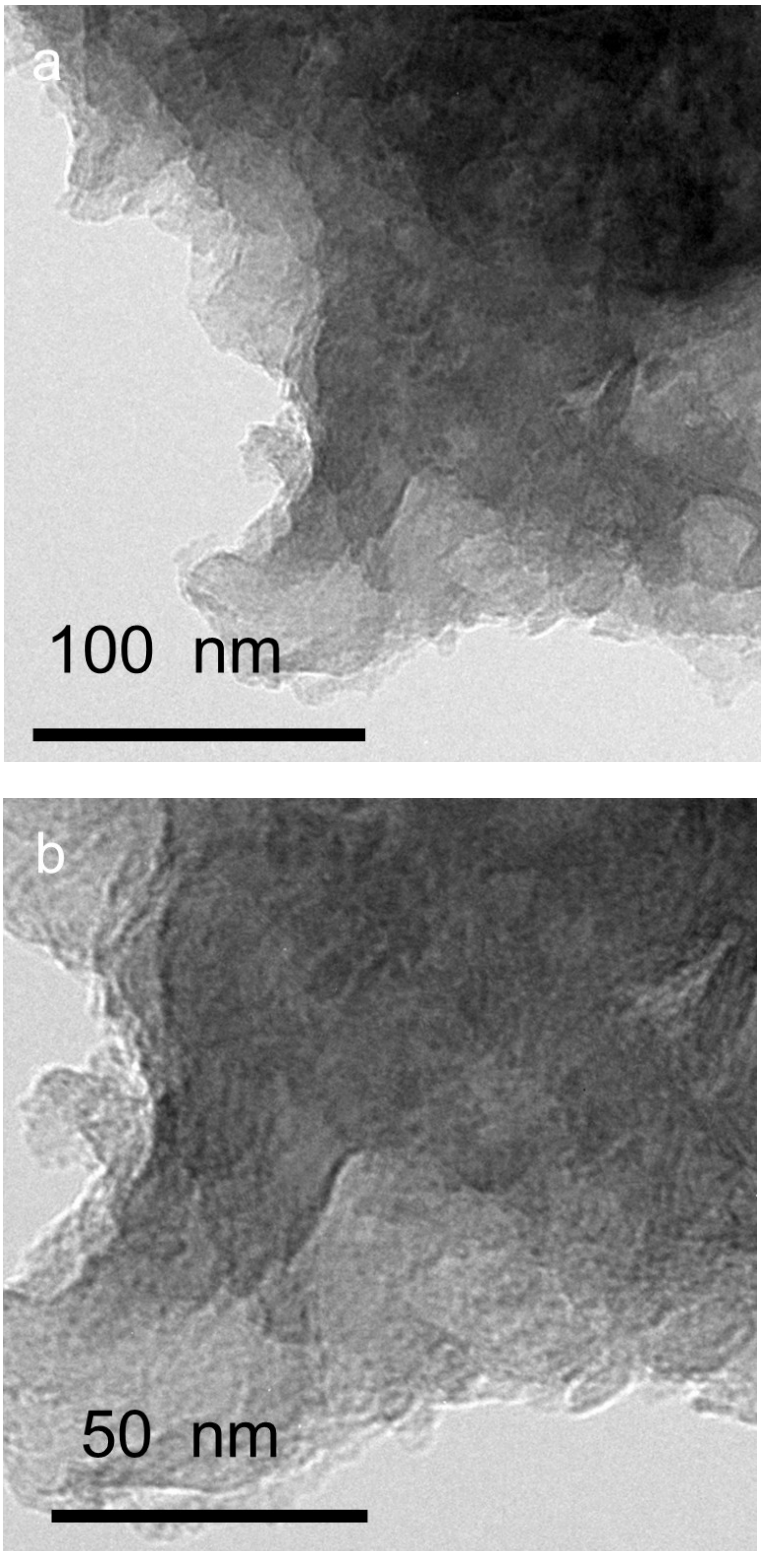

Figure S14. The high resolution TEM of Ni/CoFe LDH after OER test with different magnification.

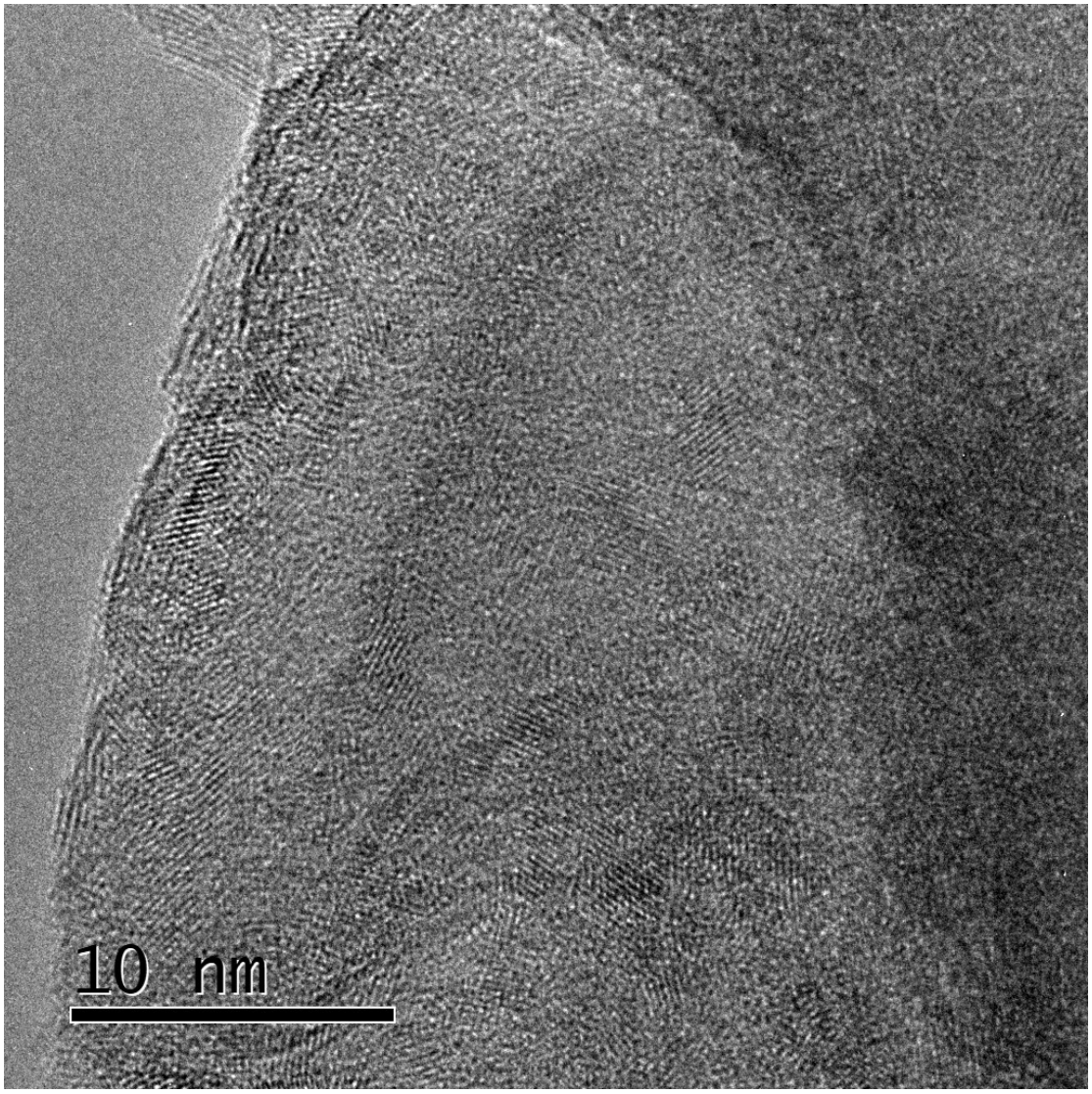

Figure S15. The HRTEM of Ni/CoFe LDH after OER test.

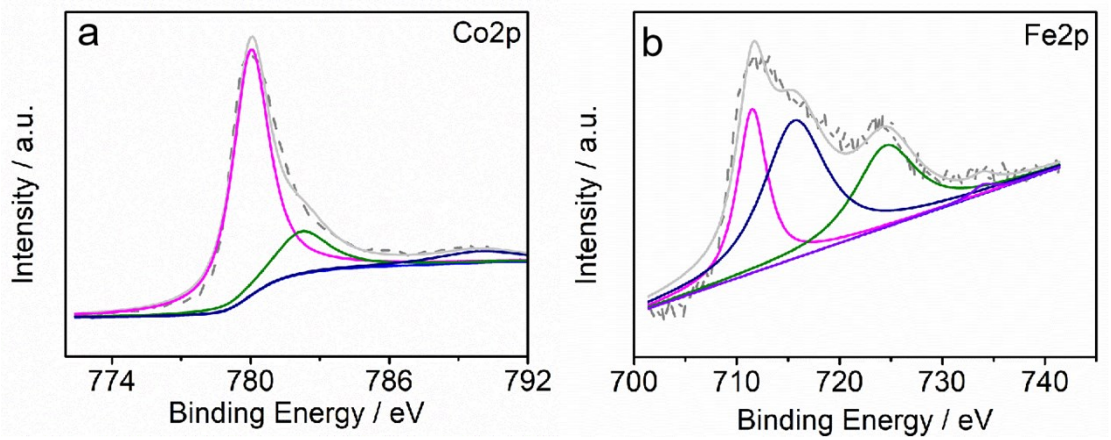

Figure S16. The high-resolution (a) Co 2p, (b) Fe 2p spectra of Ni/CoFe LDH after OER test.

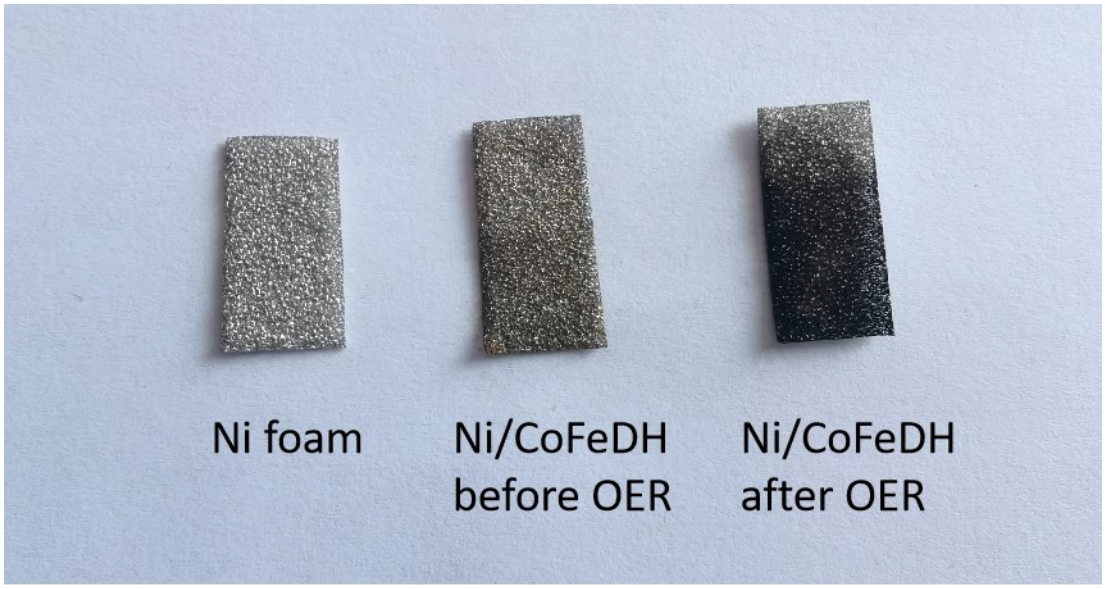

Figure S17. Optical photograph of the bare Ni foam and Ni/CoFe LDH before and after OER test.

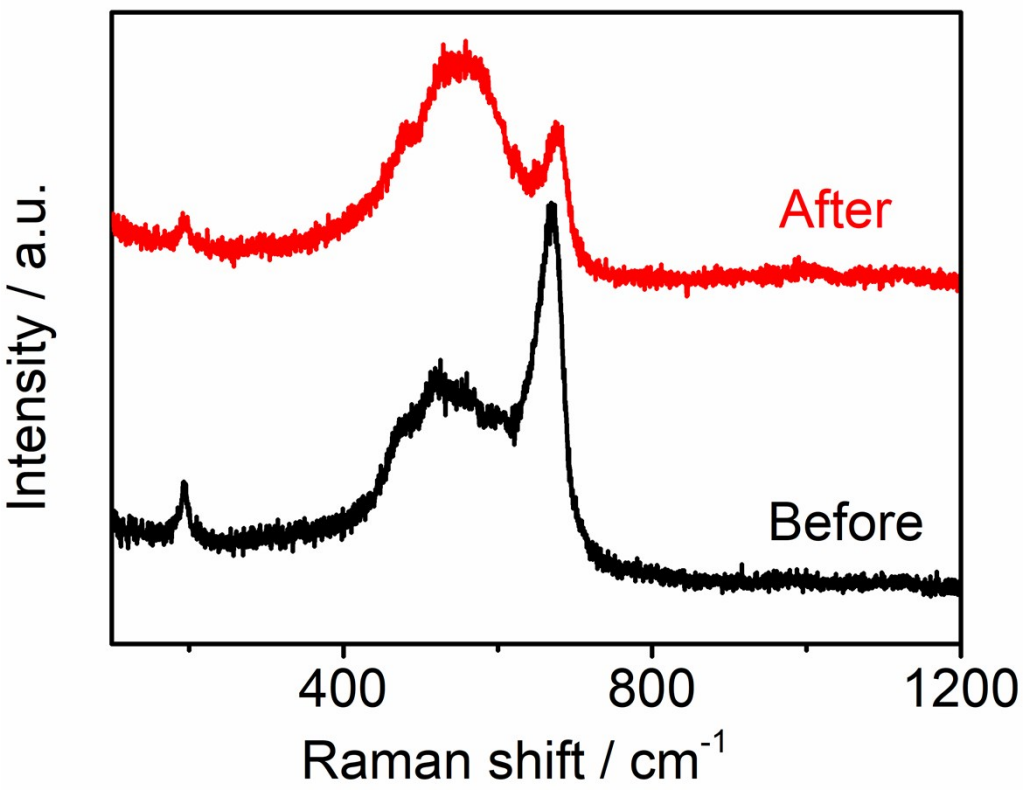

Figure S18. The Raman spectra of Ni/CoFe LDH before and after OER test.

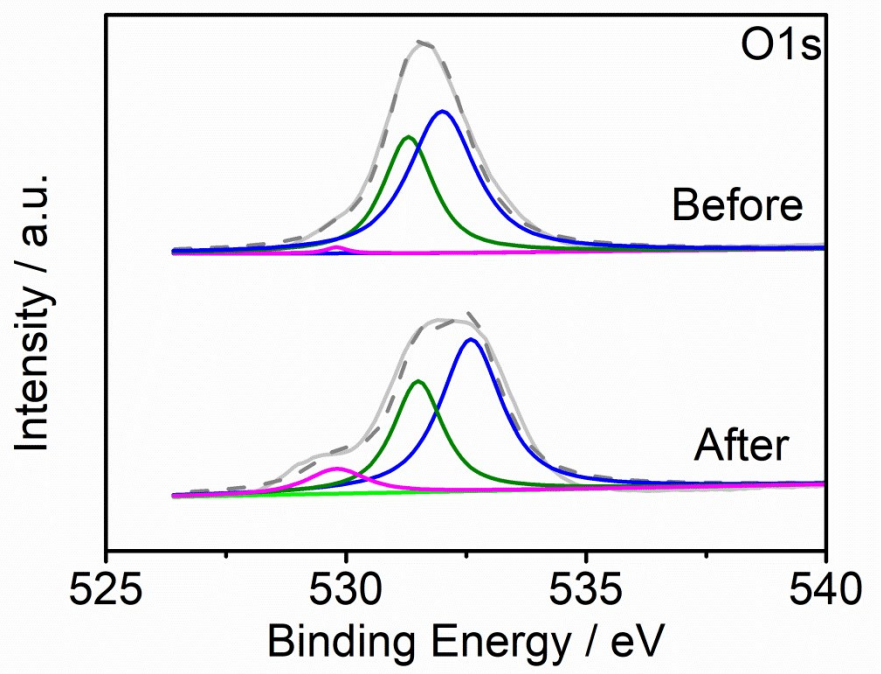

Figure S19. The high-resolution O 1s XPS spectra of Ni/CoFe LDH before and after OER test.

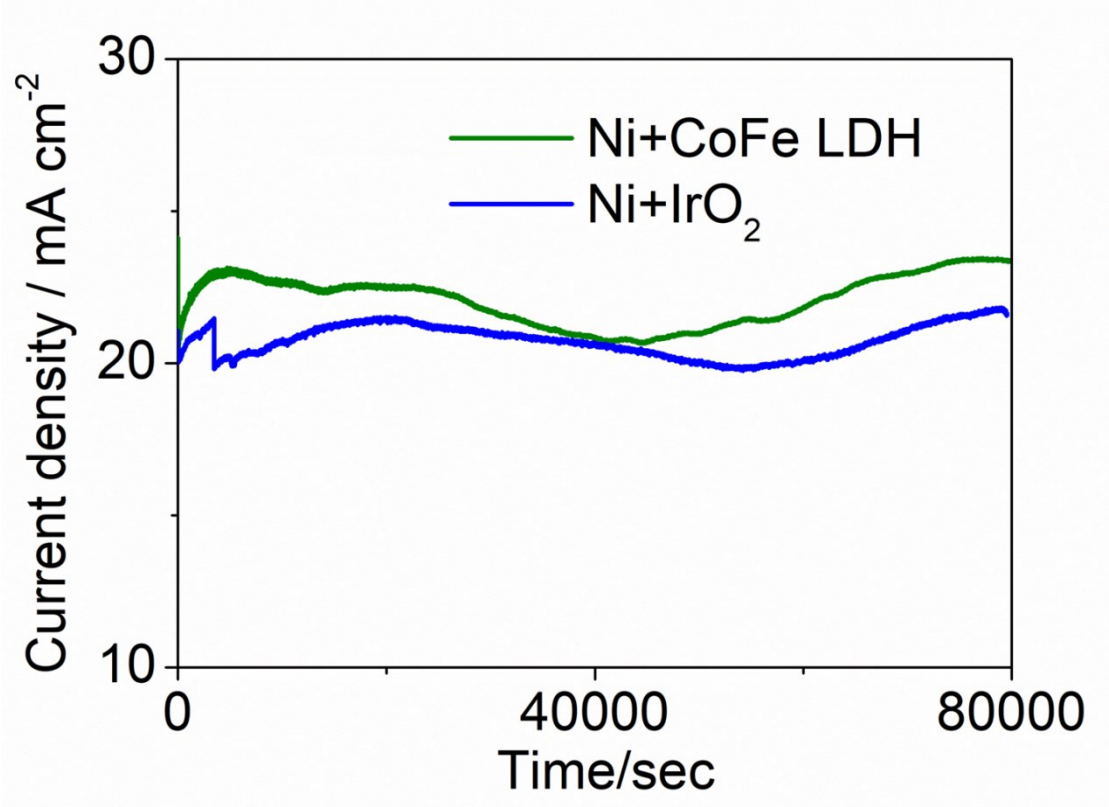

Figure S20. The i-t curve of Ni+CoFe LDH and Ni+IrO_2.

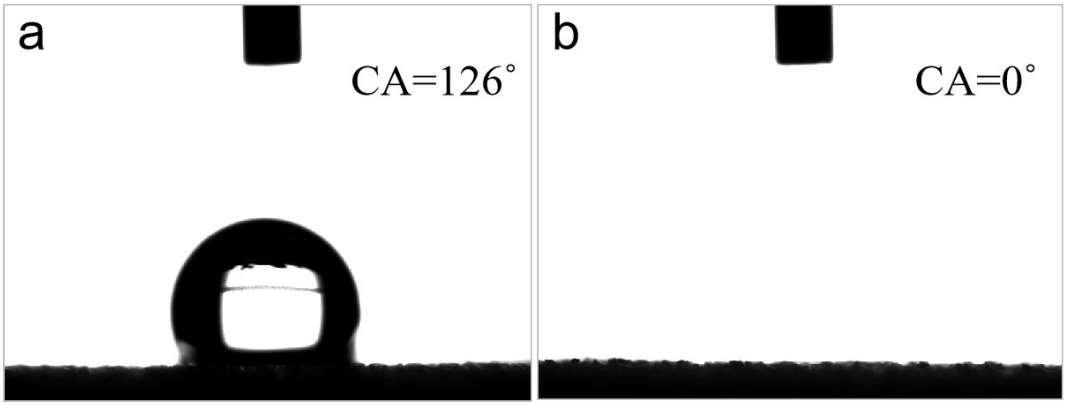

Figure S21. The wettability measurement of (a) bare Ni and (b) Ni/CoFe LDH electrodes.

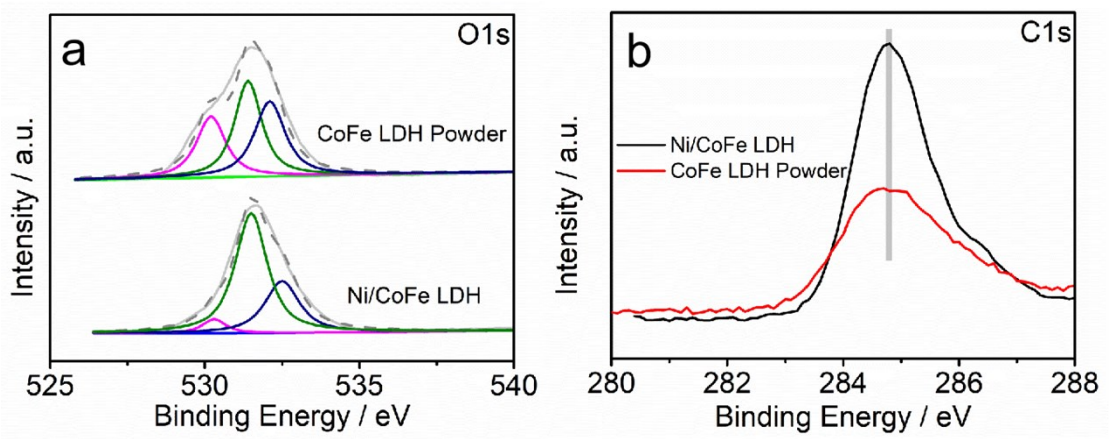

Figure S22 The high-resolution (a) O 1s, (b) C 1s spectra of Ni/CoFe LDH and CoFe LDH powder.

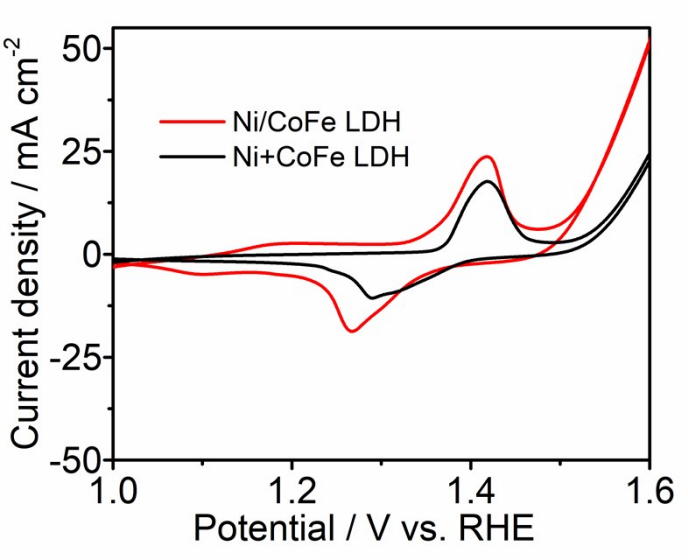

Figure S23. The CV curves of Ni/CoFe LDH and Ni+CoFe LDH .

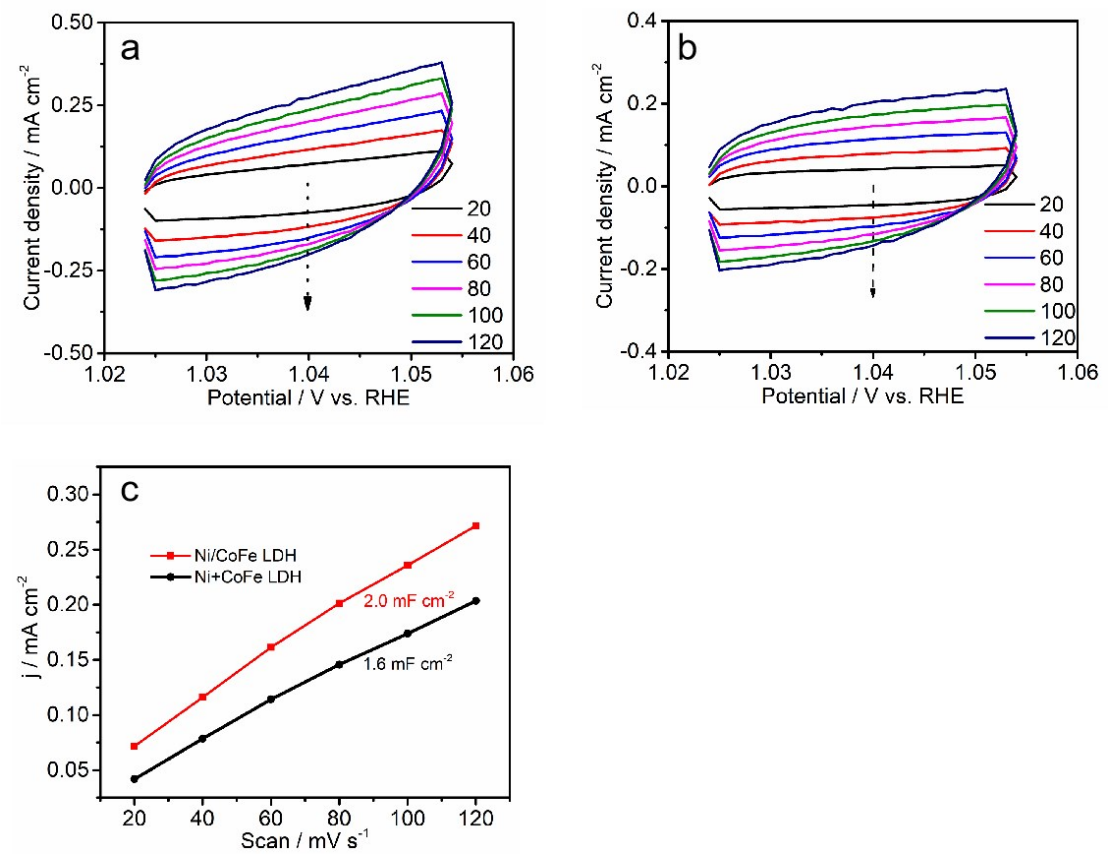

Figure S24. Investigation of the active sites. CV curves of (a) Ni/CoFe LDH and (b) Ni+CoFe LDH acquired at different scanning rates, (c) capacitive current density as a function of the scan rate.

3. Supplementary Tables

Table S1. the comparison of OER performance for some representative non-noble OER electrocatalysts.

Catalyst	Tafel slope(mV dec^{-1})	j(mA cm^{-2})	Overpotential(η/mV)	Reference
Ni/CoFe LDH	**32**	**10**	**302**	**This work**
Ni/CoFe LDH	**32**	**50**	**324**	
Ni/CoFe LDH	**32**	**100**	**333**	
Co/CoP	79.5	10	340	*Advanced Energy Materials, 2017, 7, 1602355.*
$NiFe_2O_4$	85	10	370	*Journal of Power Sources, 2019, 412, 505–513.*
$CuCo_2O_4$	67	10	400	*Journal of Power Sources, 2015, 281, 243–251.*
MOF-Ni_2P	105	10	320	*J. Mater. Chem. A, 2018, 6, 18720-18727.*
N-CG-CoO	71	10	340	*Energy Environ., 2014,7, 609-616.*
MOF-Co-B	71	10	350	*Advanced Science, 2019, 6, 1801920.*
Co_9S_8@NOSC	68	10	340	*Advanced Functional Materials, 2017, 27, 1606585.*
$NiCo_2O_4$/GNs	137	10	383	*International Journal of Hydrogen Energy,2019,44, 16120-16131*
$NiCo_{2.7}(OH)_x$	65	10	350	*Advanced Energy Materials, 2015, 5, 1401880*
MnFeCoNi alloy	83.7	10	302	*Journal of Power Sources, 2019, 430, 104–111.*
$Co_2Mo_3O_8$@NC-800	87.5	10	331	*Angew. Chem. Int. Ed., 2020, 132, 12046-12055*
NiOx/$NiCo_2O_4$/Co_3O_4	76	10	315	*Electrochimica Acta, 2019, 322, 134753.*
NCO/$Co_{0.57}Ni_{0.43}$LMOs	63	10	340	*Nanoscale, 2016, 8, 1390–1400.*
Co_3O_4	59	10	368	*Journal of Power Sources, 2016,310, 41–46.*
NiMn-LDH/ $NiCo_2O_4$	99	10	310	*Journal of Power Sources,*

				2018. 392, 23–32

4. Notes and references.

1. Dipali S. Patil, Sachin A. Pawar , Seong Hun Lee, Jae Cheol Shin, CoFe layered double hydroxide for enhanced electrochemical performance, Journal of Electroanalytical Chemistry, 2020, 862, 114012.
2. ZhongHua Xue, Hui Su, QiuYing Yu, Bing Zhang, HongHui Wang, XinHao Li, JieSheng Chen, Janus Co/CoP nanoparticles as efficient Mott-Schottky electrocatalysts for overall water splitting in wide pH range, Advanced Energy Materials, 2017, 7, 1602355.
3. A.Martínez-Lázaro, A.Rico-Zavala, F.I.Espinosa-Lagunes, JulietaTorres-González, L.Álvarez-Contreras, M.P.Gurrola, L.G.Arriaga, J.Ledesma-García, E.Ortiz-Ortega, Microfluidic water splitting cell using 3D $NiFe_2O_4$ hollow spheres, Journal of Power Sources, 2019, 412, 505–513.
4. Santosh Kumar Bikkarolla, Pagona Papakonstantinou, $CuCo_2O_4$ nanoparticles on nitrogenated graphene as highly efficient oxygen evolution catalyst, Journal of Power Sources, 2015, 281, 243–251.
5. Qin Wang, Zhengqing Liu, Hongyang Zhao, Hao Huang, Huan Jiao, Yaping Du, MOF-derived porous Ni_2P Nanosheets as novel bifunctional electrocatalysts for hydrogen and oxygen evolution reaction, J. Mater. Chem. A, 2018, 6, 18720-18727.
6. Shun Mao, Zhenhai Wen, Taizhong Huang, Yang Hou, Junhong Chen, High-performance bi-functional electrocatalysts of 3D crumpled graphene–cobalt oxide nanohybrids for oxygen reduction and evolution reactions, Energy Environ., 2014,7, 609-616.
7. Tian Wen, Yao Zheng, Jian Zhang, Kenneth Davey, ShiZhang Qiao, Co (II) Boron imidazolate framework with rigid auxiliary linkers for stable electrocatalytic oxygen evolution reaction, Advanced Science, 2019, 6, 1801920.
8. Senchuan Huang, Yuying Meng, Shiman He, Anandarup Goswami, Qili Wu, Junhao Li, Shengfu Tong, Tewodros Asefa, Mingmei Wu, N-, O-, and S-tridoped carbon-encapsulated Co_9S_8 nanomaterials: efficient bifunctional electrocatalysts for overall water splitting, Advanced Functional Materials, 2017, 27, 1606585.
9. Zesheng Li, Bolin Li, Jiaming Chen, Qi Pang, Peikang Shen, Spinel $NiCo_2O_4$ 3-D nanoflowers supported on graphene nanosheets as efficient electrocatalyst for oxygen evolution reaction, International Journal of Hydrogen Energy,2019,44, 16120-16131.
10. Jianwei Nai, Huajie Yin, Tingting You, Lirong Zheng, Jing Zhang, Pengxi Wang, Zhao Jin, Yu Tian, Juzhe Liu, Zhiyong Tang, Lin Guo, Efficient electrocatalytic water oxidation by using amorphous Ni-Co double hydroxides nanocages, Advanced Energy Materials, 2015, 5, 1401880.
11. Weiji Dai. Tao Lu, Ye Pan, Novel and promising electrocatalyst for oxygen evolution reaction based on MnFeCoNi high entropy alloy, Journal of Power Sources, 2019, 430, 104–111.
12. Zhao-Qing Liu, Ting Ouyang, Xiao-Tong Wang, Xiu-Qiong Mai, An-Na Chen, Zi-Yuan Tang, Coupling magnetic single-crystal $Co_2Mo_3O_8$ with ultrathin nitrogen-rich carbon layer for oxygen evolution reaction, Angew. Chem. Int. Ed., 2020, 132, 12046-12055.
13. Jianyue Chen, Yunhan Ling, Zhaoxia Lu, Xiaochen Huai, Fei Qin, Zhengjun Zhang, Sandwich-like $NiO_x/NiCo_2O_4/Co_3O_4$ nanoflakes enable efficient oxygen evolution

electrocatalysis, Electrochimica Acta, 2019, 322, 134753.
14. Jie Yin, Panpan Zhou, Li An, Liang Huang, Changwei Shao, Jun Wang, Hongyan Liu, Pinxian Xi, Self-supported nanoporous $NiCo_2O_4$ nanowires with cobalt–nickel layered oxide nanosheets for overall water splitting, Nanoscale, 2016, 8, 1390–1400.
15. Zhangpeng Li, Xin-Yao Yu, Ungyu Paik, Facile preparation of porous Co_3O_4 nanosheets for high-performance lithium ion batteries and oxygen evolution reaction, Journal of Power Sources, 2016,310, 41–46.
16. Liting Yang, Lin Chen, Dawen Yang, Xu Yu, Huaiguo Xue, Ligang Feng, NiMn layered double hydroxide nanosheets/$NiCo_2$ O_4 nanowires with surface rich high valence state metal oxide as an efficient electrocatalyst for oxygen evolution reaction, Journal of Power Sources, 2018. 392, 23–32.